Suplemento de la Revista Mexicana de Física **6** 011305 (2025) 1–9

Shannon entropy as an indicator for the orbital shape manipulation of a hydrogen atom under a repulsive single barrier potential

K. Das Chakladar

Department of Physics, Aliah University, Newtown, Kolkata 700160, India.

S. Mondal

Department of Chemical Sciences, Indian Institute of Science Education and Research (IISER) Kolkata, Mohanpur 741246, Nadia, India.

S. Bhattacharyya

Department of Physics, Jadavpur University, Kolkata 700032, India.

J. K. Saha

Department of Physics, Aliah University, Newtown, Kolkata 700160, India.

Received 25 February 2025; accepted 25 March 2025

The effect of a penetrable repulsive single-barrier potential on the structural properties of the hydrogen atom in ground and different excited (n, l) states $[n = 1 - 3,\ l = 0 - 2]$ is studied. The Lagrange mesh method is adopted to solve the corresponding Schrödinger equation numerically for energy eigenvalues and eigenfunctions. Different novel features and phenomena, *e.g.*, shrinking the size of the atom, atomic swelling, orbital fusion and fission, *etc.*, are noted when the strength of the barrier is changed by tuning its position and height. It is remarkable that all such alterations of the atomic orbital are well articulated from the Shannon entropy profile.

Keywords: Hydrogen atom; potential barrier; Shannon information entropy; Lagrange mesh method.

DOI: https://doi.org/10.31349/SuplRevMexFis.6.011305

1. Introduction

The structural and spectral properties of an atomic system not only undergo significant modifications under compression due to spatial confinement but also reveal several important new characteristics. The study of confined atomic systems has long been an active area of research since the pioneering works of Michels *et al.* [1] and Sommerfeld and Welker [2], where a hydrogen atom was placed under an impenetrable spherical cavity with an adjustable radius to simulate the effect of pressure and address various spectroscopic properties of astrophysical interest. Over time, researchers have explored spatially confined one-electron systems from different perspectives to develop a comprehensive understanding of confined atomic behaviour. Intriguingly, such a system also offers a potential opportunity to manipulate atomic properties by adjusting the external confinement and thereby paving the way for novel technologies based on atomic confinement. Theoretically, the confining environments can be well simulated by considering various model potentials *e.g.*, impenetrable spherical potential, spheroidal potential, open boundary potential, oscillator potential, fullerene-cage potential, potentials limited by conoidal boundaries, Debye potential, *etc.* [3–7].

Dolmatov [8, 9] demonstrated that certain semi-filled shell atoms, such as hydrogen, lithium, nitrogen, *etc.*, can undergo a transformation into exotic atomic states with significantly larger sizes and altered properties when subjected to external pressure. To model this pressure, a repulsive spherical potential with finite height and thickness was introduced. Notably, as the applied pressure increases, the atom initially behaves as expected, contracting in size. However, beyond a critical pressure threshold, an unexpected phenomenon occurs; rather than continuing to shrink, the atom undergoes a sudden expansion. This process is termed as atomic swelling. In addition to this, atoms subjected to extreme pressure may exhibit several other remarkable quantum effects, such as orbital breathing, orbital fission, orbital fusion, orbital reordering, *etc.* These effects on various atomic systems under pressure confinement, modeled using single and double barrier repulsive potentials, have been extensively studied in the literature, primarily through the analysis of orbital energy and wavefunctions [8, 9]. However, incorporating *quantum information-theoretic measures* (QIM) into such investigations could provide deeper insights into atomic properties under pressure confinement. QIM, which quantifies the statistical correlations within an atomic system, offers valuable insights into the degree of localization (or delocalization) of a quantum system. Over the years, QIM has emerged as a powerful analytical approach in various domains, including quantum entanglement, entropic uncertainty relations, electron correlation, and orbital-free density functional theory, *etc.* [10–16]. Moreover, QIM finds extensive applications in quantum information theory, quantum computing, quantum communication, teleportation, and telecommunication technologies [17–20]. The theoretical formulation of QIM relies

on several entropy-based measures, such as Shannon entropy, Fisher information, Rényi entropy, Tsallis entropy, and Onicescu informational energy [21–25]. Among these, Shannon entropy is one of the most widely used entropies, where an increase in its value signifies enhanced delocalization of the quantum system. Over the past few decades, Shannon entropy has emerged as a powerful analytical tool for characterizing various atomic and physical processes. It has been widely used as an indicator in diverse scientific domains. For instance, Shannon entropy is used to demonstrate the sorting processes in hydrothermal systems [26], to stipulate the spatial resolutions of the morphologies of the mode patterns in an optical resonator [27], a measure of the correlation and relativistic effects in confined atoms [28], to understand the atomic avoided crossings in strong parallel magnetic and electric field [29] and in static electric field [30], to justify the electron density contraction in chemical reactions [31], to designate of dynamical stability [32], as a tool to understand the age for turbulent overturns in case of the oceanic thermocline [33], *etc*.

In light of this, the present work aims at investigating the effect of *repulsive single-barrier potential* (RSB) on the (n, l) states (n and l being the principal quantum number and orbital angular quantum number, respectively) of a H atom using the *Lagrange-Laguerre mesh method* (LMM). It should be noted that the existence of a *repulsive single-barrier* (RSB) potential can naturally manifest. For instance, the presence of a repulsive barrier and the formation of a double-well potential occur naturally in free d- and f-block elements of the periodic table. Particularly, the occurrence of the repulsive barrier is due to the screening effect of the core electrons, which is the reason behind phenomena like Scandide (d-block elements) and Lanthanide contraction (f-block elements) [34, 35]. More interestingly, by appropriately choosing (V, R, Δ), it is possible to simulate various structural properties of the valence shell electrons of d-block and f-block elements. Additionally, if the systems are subjected to pressure confinement, the ordering of filling the atomic shells is altered and maintains the *aufbau* principle [34]. The strength and height of RSB potential are fixed to a specific value, while we have tuned the position of the potential within the range [0,20]. From the explicit knowledge of the wave function, we have evaluated the radial density, which is then used to compute the Shannon entropy. All the atomic effects such as swelling, orbital contraction (or compression), orbital fusion, and orbital fission are explained utilizing both the radial density and Shannon information entropy. Our particular focus is to demonstrate that the Shannon information entropy can be used as an effective indicator of all the atomic effects mentioned above. The article is organized as follows: a brief discussion of the methodology of solving the Schrödinger equation is given in Sec. 2, followed by the discussion on the results in Sec. 3. Lastly, a brief conclusion is presented in Sec. 4.

2. Methodology

2.1. The model Hamiltonian

The non-relativistic Hamiltonian (in atomic units) of a hydrogen atom under the influence of RSB potential can be written as [8, 9, 34],

$$\mathcal{H} = -\frac{1}{2}\nabla^2 + \mathcal{V}_{\text{eff}}(r) + \mathcal{V}_{\text{RSB}}(r), \tag{1}$$

where $-(1/2)\nabla^2$ is the kinetic energy of the system. $\mathcal{V}_{\text{eff.}}(r)$ is the effective coulombic potential, which can be written as,

$$\mathcal{V}_{\text{eff}}(r) = -\frac{1}{r} + \frac{l(l+1)}{2r^2}. \tag{2}$$

Here, l is the angular momentum quantum number. The RSB potential ($\mathcal{V}_{\text{RSB}}(r)$) can be written as,

$$\mathcal{V}_{\text{RSB}}(r) = \begin{cases} V & R \le r \le R + \Delta, \\ 0 & \text{Otherwise.} \end{cases} \tag{3}$$

Here (V, Δ, R) are the height, width, and the position of the repulsive barrier, respectively. As the total potential is spherically symmetric, the angular part of the wave function is given by the usual spherical harmonics $Y_l^m(\theta, \phi)$ and the radial part of the one-electron Schrödinger equation can be written as

$$-\frac{1}{2}\frac{d^2u_{nl}(r)}{dr^2} + \{\mathcal{V}_{\text{eff}}(r) + \mathcal{V}_{\text{RSB}}(r)\} \times u_{nl}(r) = Eu_{nl}(r), \tag{4}$$

where the radial function satisfies the relation $rR_{nl}(r) = u_{nl}(r)$ and obeys the normalization condition

$$\int_0^\infty r^2 R_{nl}^2(r)\, dr = \int_0^\infty u_{nl}^2(r)\, dr = 1. \tag{5}$$

2.2. Lagrange mesh method

The radial wavefunction is expanded in terms of the regularized Lagrange functions, defined within the range $(0, \infty)$ [36] as

$$u_{nl}(r) = \sum_k C_{nl}^k f_k(r). \tag{6}$$

The Lagrange functions are a set of orthogonal functions associated with the Gauss Quadrature

$$f_i(r_j) = \frac{1}{\sqrt{\lambda_i}}\delta_{i,j}. \tag{7}$$

Here λ_i are the weight factors associated with the Gauss-Laguerre Quadrature within the specified range. Thus, any integral within the aforementioned range can be solved using the Gauss quadrature method,

$$\int_0^\infty u_{nl}(r)\, dr = \sum_{k=1}^{N} \lambda_k u_{nl}(r_k), \tag{8}$$

where the mesh points (r_k) are chosen as the roots of the Laguerre Polynomial ($L_N(r_k) = 0$) of degree N. The orthogonality of the Lagrange function can be tested using Eqs. (8) and (7) as

$$\int_0^\infty f_i(r) f_j(r)\, dr = \sum_{k=1}^{N} \lambda_k f_i(r_k) f_j(r_k) = \delta_{i,j}. \quad (9)$$

In this study, the mathematical expression of $f_i(r)$ has been taken as [36, 37]

$$f_i(r) = (-1)^i \sqrt{r_i} \frac{L_N(r)}{r - r_i} e^{-\frac{r}{2}}. \quad (10)$$

Using Eq. (7), the expression for λ_i can be extracted as,

$$\lambda_i = \frac{e^{r_i}}{r_i \{L'_N(r_i)\}^2}, \quad (11)$$

where, $L'_N(r_i)$ is the first derivative of Laguerre Polynomial of degree N at $r = r_i$. Due to the present singularity of the $\mathcal{V}_{\texttt{eff.}}(r)$ at $r = 0$, a Lagrange function must be regularized as [36, 38],

$$\tilde{f}_j(r) = \left(\frac{r}{r_j}\right)^{n_0} f_j(r). \quad (12)$$

Due to the regularization, the orthogonality of the Lagrange function becomes inexact for $n_0 > 1/2$, which does not alter the accuracy of the method.

Using Eqs. (6) and (7) in Eq. (4), we get,

$$\sum_i^N (T_{ij} + \mathcal{V}_{ij}) C^i_{nl} = E C_j. \quad (13)$$

Here, T_{ij} is the kinetic energy element. The off-diagonal kinetic energy elements ($T_{i\neq j}$) can be written as [36],

$$T_{i\neq j} = \frac{(-1)^{i-j+1}}{(r_i - r_j)^2} \left(\frac{r_j^{n_0-\frac{3}{2}}}{r_i^{n_0-\frac{1}{2}}}\right) \times \{(2n_0 - 3) r_j - (2n_0 - 1) r_i\}, \quad (14)$$

and the diagonal kinetic energy elements (T_{ii}) take the form

$$T_{ii} = \frac{1}{12 r_i^2}(-12 n_0^2 + 24 n_0 - 8 + (4N + 2) r_i - r_i^2). \quad (15)$$

The potential energy elements ($\mathcal{V}_{ij}$) can be written as [36],

$$\mathcal{V}_{ij} = \{\mathcal{V}_{\text{eff}}(r_i) + \mathcal{V}_{\text{RSB}}(r_i)\}\delta_{ij}. \quad (16)$$

Now, using the matrix representation of the quantum mechanical operators, Eq. (1) can be solved as

$$\underline{\underline{\mathcal{H}}}\, \underline{\mathcal{C}} = E\, \underline{\mathcal{C}}, \quad (17)$$

here, $\underline{\mathcal{C}}$ is defined as $\underline{\mathcal{C}} = [C_1, C_2, C_3 \ldots, C_N]^T$.

3. Results and discussion

The main objective of this study is to utilize the concept of Shannon entropy to understand various intuitive phenomena, such as atomic swelling, orbital fission, orbital fusion, *etc.* The parameters defining the height (V), width (Δ), and position (R) of the RSB potential are chosen carefully following the work of Dolmatov *et al*. [9]. In their study, the authors demonstrated that the atomic swelling occurs for the ground state of the hydrogen atom for potential parameters $(V, R, \Delta) = (2.5, 1.45, 5.0)$ a.u. However, such a swelling of ground state atomic orbital for the hydrogen atom may also occur for any value of $V > 2.5$ a.u. and $\Delta > 1.0$ a.u., irrespective of R. Therefore, we have fixed the value of Δ and V at 5.0 and 4.0 a.u., respectively, throughout our calculation, while the position of the barrier (R) is varied gradually. Our analysis reveals that the LMM has an accuracy of up to 14 decimal places for $N > 100$. In this investigation, the value of N is fixed between 300 and 360, depending upon the states under consideration.

Next, the radial Shannon entropy of the system in position space is calculated as

$$S_r = \int_0^\infty r^2 \rho_{nl}(r) \ln \rho_{nl}(r) dr \approx \sum_k \lambda_k r_k^2 \rho_{nl}(r_k) \ln \rho_{nl}(r_k), \quad (18)$$

where $\rho_{nl}(r) = R^2_{nl}(r)$. As the external potential does not alter the angular distribution of the wavefunction, we have taken the values of the angular part of the Shannon entropy ($S_{\theta,\phi}$) in position space directly from Jiao *et al.* [39]. Thus, the total Shannon entropy in position space is defined as

$$\mathbf{S}_r = S_r + S_{\theta,\phi}. \quad (19)$$

Shannon entropy is the measure of the total 'information' ($I = -\log \rho$) [21] content of a system that provides an intuitive description of the delocalization of the electronic probability density. At $R = 100.0$ a.u., where the system becomes asymptotically free, the value of the Shannon entropy ($\mathbf{S}_r$) for the $1s$ state of the hydrogen atom becomes 4.14473 a.u., which is similar to the findings of Jiao *et al.* [39]. As the value of R decreases the variation of Shannon entropy showcases various interesting phenomena, such as atomic swelling, orbital fusion, orbital fission, orbital collapse, *etc.*

The values of energy ($-E$) and $\mathbf{S}_r$ *w.r.t.* the position of the barrier (R) for different nl states of the hydrogen atom are given in Table I. As mentioned, for the $1s$ state of the hydrogen atom, the value of Shannon entropy becomes 4.14473 a.u. When R decreases to 2.0 a.u., Shannon entropy also decreases to 2.86855 a.u., which is about 69.2% less than the former. This signifies that the amount of delocalization of the $1s$-electron density decreases, *i.e.* becomes more localized at $R = 2.0$ a.u. compared to $R = 100.0$ a.u. However, at $R = 1.48$ a.u., the value of $\mathbf{S}_r$ for the $1s$ state of the hydrogen atom abruptly increases to 10.15506 a.u., which is nearly 2.45 times higher than the value of $\mathbf{S}_r$ at $R = 100.0$ a.u. This

TABLE I. The value of E and $\mathbf{S}_r$ for nl ($n = 1-3$ and $l = 0-2$) states of the Hydrogen atom for different values of R. All quantities are specified in atomic units. The value of V, Δ is fixed at $V = 4.0$ a.u., $\Delta = 5.0$ a.u. For comparison purposes, the values of $\mathbf{S}_r$ are taken from † Jiao *et al.* [39], ° Mondal *et al.* [40].

R	$1s$		$2s$		$2p$		$3s$		$3p$		$3d$	
	$-E$	$\mathbf{S}_r$	$-E$	$\mathbf{S}_r$	$-E$	$\mathbf{S}_r$	$-E$	$\mathbf{S}_r$	$-E$	$\mathbf{S}_r$	$-E$	$\mathbf{S}_r$
100.00	0.50000	4.14473	0.12500	8.11098	0.12500	7.26490	0.05556	10.42653	0.05556	9.80582	0.05556	9.34563
		4.14473†		8.11093†		7.26490†		10.42648†		9.80585†		9.34563†
		4.14(+0)°		8.11(+0)°		7.26(+0)°		1.04(+1)°		9.81(+0)°		9.35(+0)°
20.00	0.50000	4.14473	0.12499	8.10766	0.12500	7.26324	0.05110	9.80819	0.05245	9.27826	0.05432	9.02515
18.00	0.50000	4.14473	0.12496	8.09784	0.12498	7.25799	0.04629	9.52403	0.04901	9.01531	0.05285	8.83471
16.00	0.50000	4.14473	0.12482	8.06831	0.12492	7.24090	0.03742	9.18575	0.04264	8.69552	0.05005	8.59251
14.36	0.50000	4.14473	0.12429	7.99715	0.12467	7.19592	0.02668	12.58789	0.03138	8.32457	0.04499	8.30160
14.00	0.50000	4.14473	0.12429	7.99715	0.12467	7.19592	0.02750	12.50328	0.03138	8.32457	0.04499	8.30160
13.74	0.50000	4.14473	0.12393	7.95962	0.12450	7.17080	0.02750	12.50328	0.02634	12.12440	0.04256	8.19438
12.00	0.50000	4.14473	0.12266	7.85853	0.12388	7.09992	0.03020	12.24070	0.02878	11.86904	0.03617	7.96515
10.80	0.50000	4.14470	0.11827	7.63319	0.12166	6.93088	0.03119	12.15008	0.02968	11.78117	0.02676	11.86190
10.00	0.50000	4.14467	0.11568	7.53715	0.12033	6.85584	0.03333	11.96384	0.03158	11.60099	0.02824	11.69603
8.00	0.49999	4.14334	0.09410	7.04559	0.10924	6.45852	0.03700	11.67097	0.03480	11.31896	0.03064	11.43987
6.48	0.49976	4.12774	0.03980	11.46581	0.07890	5.91101	0.03422	6.38024	0.03723	11.12247	0.03239	11.26434
6.00	0.49952	4.11582	0.04133	11.35999	0.06565	5.75181	0.02385	12.92492	0.03853	11.02152	0.03330	11.17524
5.25	0.49829	4.07002	0.04466	11.14139	0.04135	10.81390	0.02536	12.74716	0.02785	5.40737	0.03521	10.99461
4.00	0.49095	3.90868	0.04843	10.91273	0.04448	10.59823	0.02703	12.56275	0.02530	12.24566	0.03724	10.81122
2.00	0.30782	2.86856	0.05764	10.42090	0.05186	10.14064	0.03094	12.17165	0.02855	11.88439	0.04157	10.44020
1.48	0.06330	10.15506	0.03324	11.96371	0.05621	9.89769	0.02078	13.29118	0.03040	11.69575	0.04383	10.25587
1.00	0.06647	10.01645	0.03449	11.85633	0.05857	9.77247	0.02141	13.20381	0.03138	11.59942	0.04497	10.16509

symbolizes that the system has become even more delocalized than the asymptotic (free) case, indicating the emergence of the phenomenon called atomic swelling [8]. From Fig. 1a), it is evident that, at $R = 1.48$ a.u., the entire electronic cloud tunnels through the repulsive barrier and the atomic system becomes 'swelled'. As a result of this, the $1s$ probability density becomes extended beyond 20 a.u. [see Fig. 1a)]. The critical value of $R = R_c$ at which the atomic swelling occurs strongly depends on the principal quantum number n and angular momentum l. After the swelling of the $1s$-electron density, if the value of R ($\leq R_c$) decreases even more, the value of $\mathbf{S}_r$ decreases quite marginally. For example, at $R = 1.0$ a.u., we find $\mathbf{S}_r = 10.01645$ a.u., pointing to slight localization. This can be understood from the fact, that by introducing the repulsive barrier, the effective coulombic potential is divided into two attractive wells, *e.g.*, inner-well and outer-well. As the value of R decreases, the strength of the inner-well decreases while the strength of the outer-well increases [8] which is also the reason behind the atomic swelling. When the value of R is reduced further after the swelling ($R < R_c = 1.48$ a.u.), due to the increased strength of the outer-well, the electronic cloud becomes slightly localized, which is reflected in Fig. 1b). It is also necessary to mention that, as we are employing the Lagrange's mesh method over a fixed Laguerre mesh of dimension N, any spatial point that comes between two discrete mesh points, becomes invisible to the method. That is why the step-like feature of the variation of $\mathbf{S}_r$ appears. However, it does not affect the overall feature of variation as the points are closely spaced and distributed over the space. Also, the step-like feature can be removed by scaling the mesh accordingly.

For excited states of s-symmetry, such as $2s$ and $3s$ states of the hydrogen atom, more exquisite phenomena can be seen. For example, in Fig. 2b), the variation of the Shannon entropy of the $2s$ state exhibits the first abrupt change at $R = 6.48$ a.u., indicating the atomic swelling. However, from Fig. 2a), we can see that in the swelled hydrogen atom in the $2s$ state, the characteristic two lobes are fused and the probability distribution assumes $1s$ characteristics with a single distinct lobe. This phenomenon is known as orbital fusion [9]. At $R = 6.48$ a.u., the Shannon entropy of the system becomes 11.46581 a.u., which is 1.4 times higher than the Shannon entropy of the asymptotically free $2s$ state ($\mathbf{S}_r = 8.11098$ a.u. at $R = 100.0$ a.u.), which demonstrates the atomic swelling. As the value of R is further reduced, two extremely strange yet intuitive phenomena appear. First,

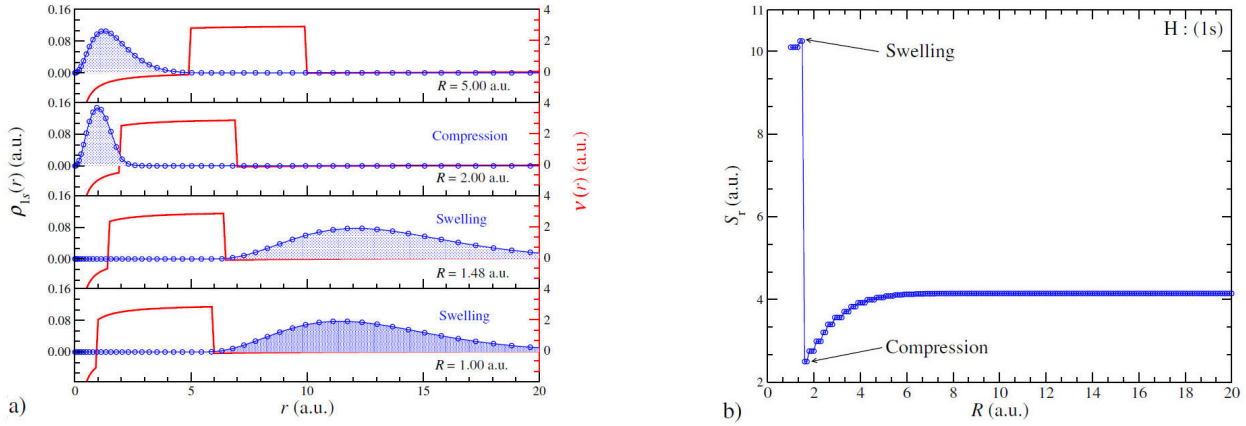

FIGURE 1. a) Radial density (ρ_{nl}) vs. radial distance (r) (the red line represents the total potential $[\mathcal{V}(r) = \mathcal{V}_{\texttt{eff.}}(r) + \mathcal{V}_{\texttt{RSB}}(r)]$ with $V = 4.0$ a.u., $\Delta = 5.0$ a.u. fixed for $\mathcal{V}_{\texttt{RSB}}(r)$) and b) Shannon entropy ($\mathbf{S}_r$) vs. position of the repulsive barrier (R) for the ground ($1s$) state of hydrogen atom.

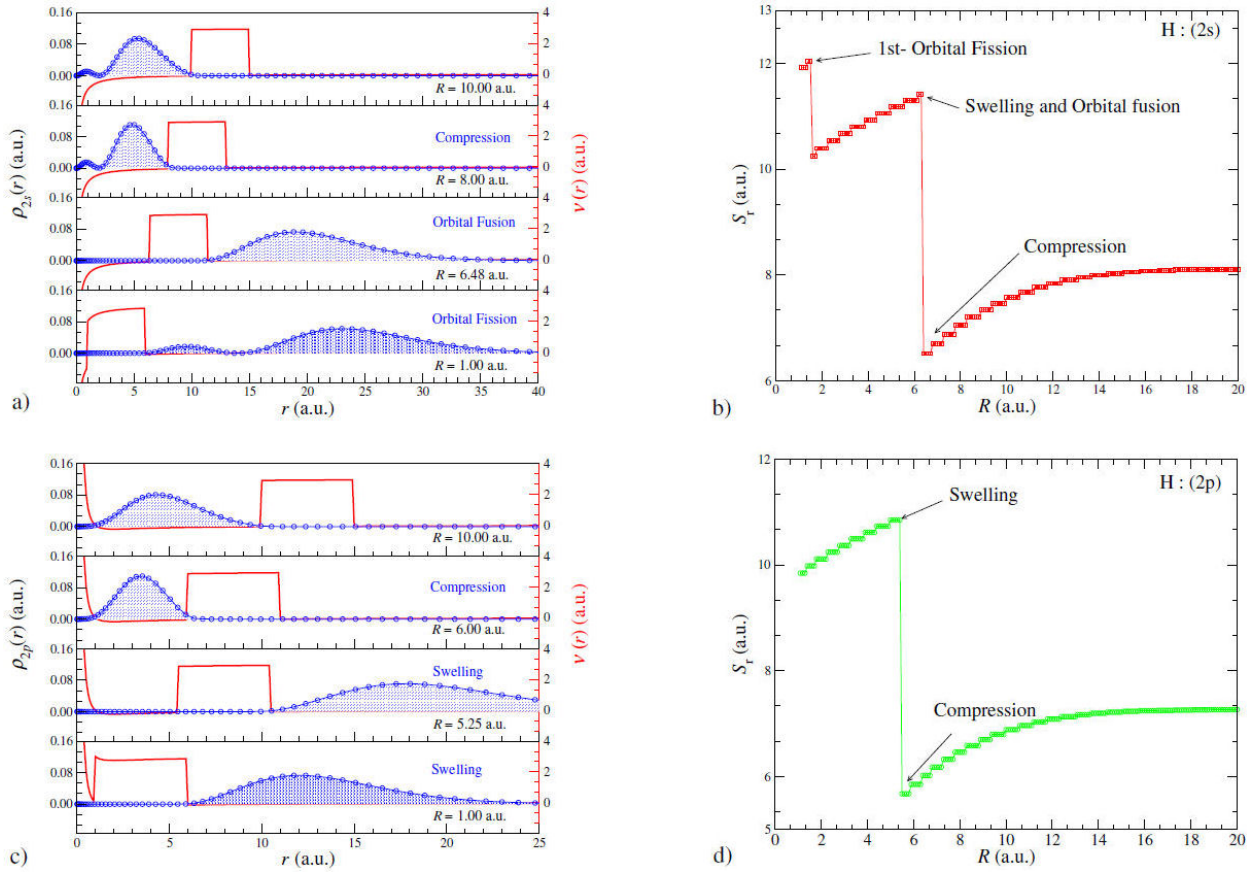

FIGURE 2. a), c) Radial density ρ_{nl} vs. radial distance r (the red line represents the total potential $[\mathcal{V}(r) = \mathcal{V}_{\texttt{eff.}}(r) + \mathcal{V}_{\texttt{RSB}}(r)]$ with $V = 4.0$ a.u., $\Delta = 5.0$ a.u. fixed for $\mathcal{V}_{\texttt{RSB}}(r)$) and b), d) Shannon entropy $\mathbf{S}_r$ vs. position of the repulsive barrier R for the excited $2s$ and $2p$ states of hydrogen atom.

at $R = 1.48$ a.u., the variation of the Shannon entropy of the $2s$ state [see Fig. 2a)-2b)] exhibits another abrupt change. As we can see, at $R = 1.48$ a.u. the value of Shannon entropy becomes $\mathbf{S}_r = 11.96371$ a.u. from $\mathbf{S}_r = 10.28980$ a.u. corresponding to $R = 1.5$ a.u., indicating the release of the fusion of two lobes of the $2s$ state *or,* first orbital fission. Second, the value of $\mathbf{S}_r$ at $R = 1.5$ a.u. becomes approximately equal to the value of $\mathbf{S}_r$ of $1s$ state at $R = 1.48$ a.u. This indicates that the characteristic of the swelled atom in the $2s$ state becomes almost similar to the characteristics of the swelled $1s$ state, just before the first orbital fission appears. Interestingly enough, at $R = 1.5$ a.u., the value of E_{2s} becomes -0.06037 a.u., approximately close to $E_{1s} = -0.06330$ a.u.

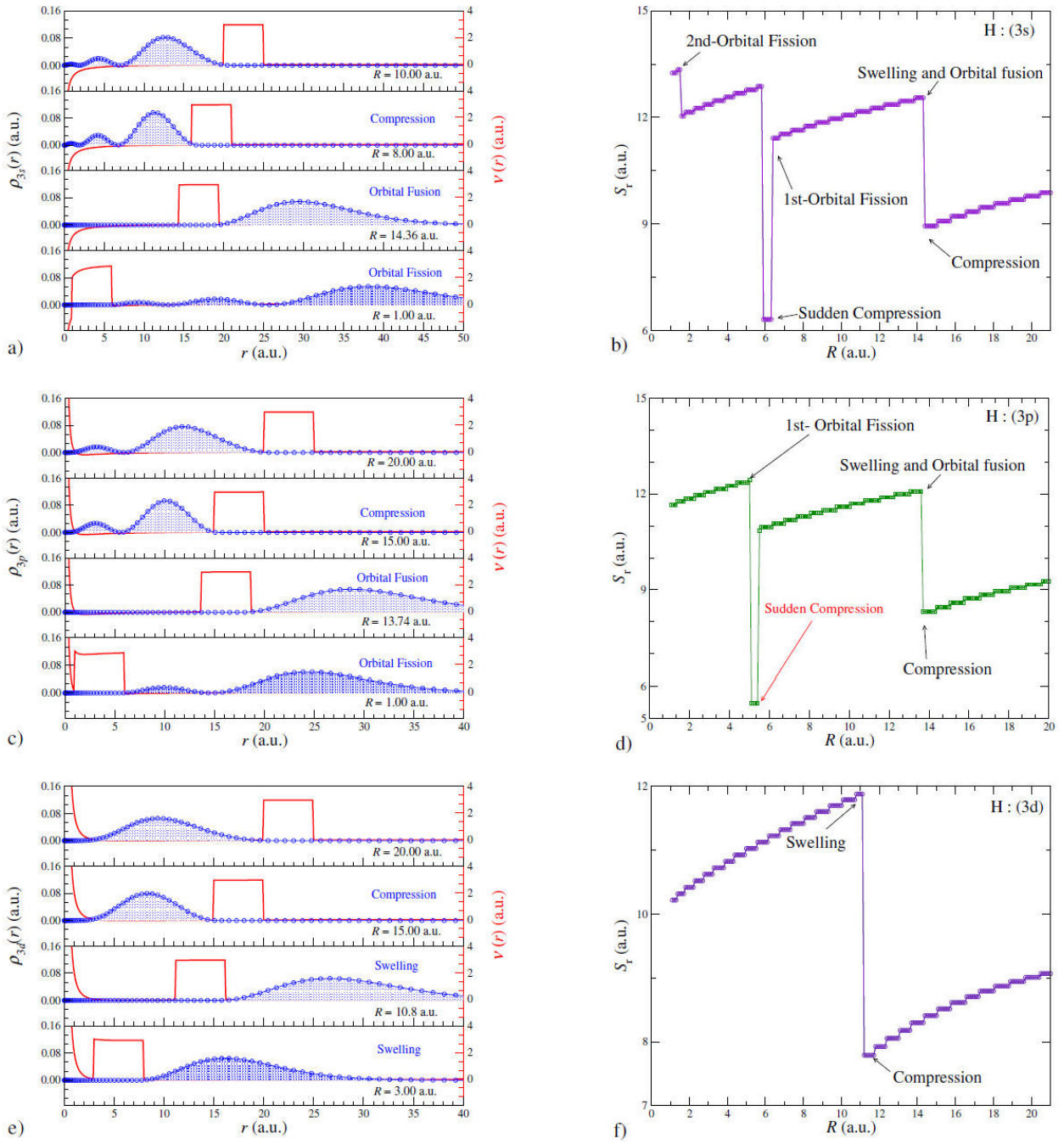

FIGURE 3. a), c), e) Radial density profile ρ_{nl} vs. radial distance r (the red line represents the total potential $[\mathcal{V}(r) = \mathcal{V}_{\texttt{eff.}}(r) + \mathcal{V}_{\texttt{RSB}}(r)]$ with $V = 4.0$ a.u., $\Delta = 5.0$ a.u. fixed for $\mathcal{V}_{\texttt{RSB}}(r)$) and b), d), f) Shannon entropy $\mathbf{S}_r$ vs. position of the repulsive barrier R for the excited $3s$, $3p$ and $3d$ states of hydrogen atom.

at $R = 1.48$ a.u., indicating further similarity between the swelled $1s$ and $2s$ states.

Similarly, for the $3s$ state, the swelling occurs at $R = 14.36$ a.u., where the distinct lobes of the $3s$ state are fused to attain a single lobe of $1s$ characteristics. At $R = 14.36$ a.u., the value of $\mathbf{S}_r$ for $3s$ state becomes 12.58789 a.u., *i.e.*, 1.2 times higher than $\mathbf{S}_r = 10.42653$ a.u. at $R = 100.0$ a.u. As R decreases, the value of $\mathbf{S}_r$ experiences a sudden drop to 6.38024 a.u. at $R = 6.48$ a.u., indicating a sudden strong localization [see Fig. 3b)]. Also, at $R = 6.48$ a.u. the first orbital fission of the $3s$ state appears. Interestingly, just before the first orbital fission ($R = 6.5$ a.u.), the $\mathbf{S}_r$ of swellen $3s$ state becomes 11.4681 a.u., exactly similar to the value of $\mathbf{S}_r$ for swelled $2s$ state at $R = 6.48$ a.u. Also, at $R = 1.48$ a.u., another abrupt change can be seen in Fig. 3b), indicating second orbital fission [see Fig. 3a)].

Atomic swelling can also be observed for $l \neq 0$ states of hydrogen atoms as well. In case of the $l = 1$ and $l = 2$ angu-

lar momentum states, $2p$ and $3d$ states have single lobe distribution [see Fig. 2c) and 3e)]. For the $2p$ state, the swelling occurs at $R = 5.25$ a.u. at which the variation of Shannon entropy *w.r.t.* R exhibits an abrupt change from 5.58391 a.u. measured at $R = 5.3$ a.u. to 10.81390 a.u. at $R = 5.25$ a.u. [see Fig. 2d)]. Similarly, for the $3d$ state, atomic swelling occurs at $R = 10.8$ a.u. [see Fig. 3f)]. Moreover, for the $3p$ state, which has two distinct lobes, the variation of Shannon entropy *w.r.t.* R showcases three fascinating phenomena [see Figs. 3c)-3d)]. First, at $R = 13.74$ a.u. the $3p$ state exhibits atomic swelling and the two characteristic lobes fused together. Next, at $R = 5.25$ a.u., a sudden compression of the $3p$ state occurs, which can be seen by the sharp decrement of $\mathbf{S}_r$: from $\mathbf{S}_r = 10.81390$ a.u. at $R = 5.3$ a.u. to $\mathbf{S}_r = 5.407367$ a.u. at $R = 5.25$ a.u [see Fig. 3d)]. This a sudden compression is also known as orbital collapse [34], prevalent in $l \neq 0$ states. During the orbital collapse, the value of $\mathbf{S}_r$ lowers by 55.1% as compared to the value of $\mathbf{S}_r = 9.80582$ a.u. at $R = 100.0$, indicating strong localization. Last, at $R = 4.9$ a.u. the first orbital fission occurs for the $3p$ state, indicated by another abrupt change in the value of $\mathbf{S}_r$.

4. Conclusions

In this article, Shannon entropy in position space has been exploited to understand various intuitive atomic phenomenon, such as atomic swelling, orbital fission, orbital fusion, orbital collapse, *etc.* of a hydrogen atom trapped inside a repulsive barrier of fixed width and height. By modulating the position of the barrier and analyzing the subsequent alteration of the information entropy, the aforementioned exotic phenomena can be realized. In order to solve the Schrödinger equation for the system under consideration, the Lagrange mesh method (LMM) is employed over an extremely precise Gauss-Laguerre mesh. The radial part of the Shannon entropy is calculated using the Gauss quadrature method and the values of the angular part of the Shannon entropy are taken from literature. The variations of the Shannon entropy for nl states ($n = 1 - 3$ and $l = 0 - 2$) of a hydrogen atom *w.r.t.* the position of the repulsive barrier have revealed some exquisite features related to the mentioned exotic phenomena. For example, as the value of R is gradually lowered, at a certain value of R the variation of $\mathbf{S}_r$ exhibits a single abrupt increment for $1s$ ($R = 1.48$ a.u.), $2p$ ($R = 5.25$ a.u.) and $3d$ ($R = 10.8$ a.u.) states, indicating strong delocalization of the single-lobe probability density. This is known as atomic swelling. For multi-lobe distributions, more exquisite features can be seen. For example, for a hydrogen atom in $2s$ and $3s$ states, the atomic swelling can be observed by studying the first abrupt increment in the value of Shannon entropy at $R = 6.48$ a.u. and $R = 14.36$ a.u. However, if the value of R is gradually lowered, the variations of $\mathbf{S}_r$ exhibit more abrupt increments, demonstrating first orbital fission ($R = 1.48$ a.u. for $2s$ state, $R = 6.48$ a.u. for $3s$ state) and second orbital fission ($R = 1.48$ a.u. for $3s$ state). The first orbital fission can also be observed for the $3p$ state at $R = 4.9$ a.u. For $3s$ and $3p$ states, the variations of $\mathbf{S}_r$ exhibit sudden decrement, signalling strong localization, known as orbital collapse. Shannon entropy can also be used to realize the similarity between two swelled atomic states. For example, at $R = 1.5$ a.u., *i.e.*, just before the first orbital fission occurs in the $2s$ state, the Shannon entropy of the swelled $2s$ state becomes almost equal to the Shannon entropy of the swelled $1s$ state, suggesting pressure-induced quantum similarity. The same phenomena can also be observed between swelled $2s$ and $3s$ states as well. Overall, the Shannon entropy can be used as an extremely powerful tool to analyze such convoluted phenomena in terms of information theory.

Acknowledgments

Jayanta K. Saha acknowledges partial financial support from Science and Engineering Research Board (SERB), Govt. of India under file number CRG/2022/003547

1. A. Michels, J. De Boer, and A.Bijl, Remarks concerning molecular interaction and their influence on the polarisability, *Physica* **4** (1937) 981, https://doi.org/10.1016/S0031-8914(37)80196-2

2. A. Sommerfeld and H. Welker, Künstliche Grenzbedingungen beim Keplerproblem, *Ann. Phys.* **424** (1938) 56, https://doi.org/10.1002/andp.19384240109

3. J. Sabin and E. Brandas, eds., Advances in Quantum Chemistry, vol. **58** (Academic Press, 2009), https://doi.org/10.1016/S0065-3276(09)00701-1

4. J. Sabin and E. Brändas, Advances in Quantum Chemistry: Theory of Confined Quantum Systems - Part Two, **58** of Advances in Quantum Chemistry, 1-297 *(Academic Press, 2009)*. https://doi.org/10.1103/PhysRevA.110.042819

5. S. Mondal, A. Sadhukhan, K. Sen, and J. K. Saha, Stability of a two-electron system under pressure confinement: structural and quantum information theoretical analysis, *J. Phys. B: At., Mol. Opt. Phys.* **56** (2023) 155001, https://doi.org/10.1088/1361-6455/ace177

6. K. D. Chakladar, S. Mondal, K. Sen, and J. K. Saha, Quantum-information-theoretic analysis of Zee systems under pressure confinement, *Phys. Rev. A* **110** (2024) 042819, https://doi.org/10.1103/PhysRevA.110.042819

7. S. Mondal, A. Sadhukhan, J. K. Saha, and A. K. Roy, Information-theoretic measures and Compton profile of H atom under finite oscillator potential, *J. Phys. B: At., Mol.*

Opt. Phys. **57** (2024) 175001, https://dx.doi.org/10.1088/1361-6455/ad5fd3

8. V. Dolmatov and J. King, Atomic swelling upon compression, *J. Phys. B: At., Mol. Opt. Phys.* **45** (2012) 225003, https://dx.doi.org/10.1088/0953-4075/45/22/225003
9. V. K. Dolmatov, Confinement-induced orbital breathing, fusion, fission and re-ordering in semifilled shell atoms, *J. Phys. B: At., Mol. Opt. Phys.* **46** (2013) 095005, https://dx.doi.org/10.1088/0953-4075/46/9/095005
10. A. Nahum, J. Ruhman, and D. A. Huse, Dynamics of entanglement and transport in one-dimensional systems with quenched randomness, *Phys. Rev. B* **98** (2018) 035118, https://doi.org/10.1103/PhysRevB.98.035118
11. H. Barghathi, C. M. Herdman, and A. Del Maestro, Rényi Generalization of the Accessible Entanglement Entropy, *Phys. Rev. Lett.* **121** (2018) 150501, https://doi.org/10.1103/PhysRevLett.121.150501
12. P. Lévay, S. Nagy, and J. Pipek, Elementary formula for entanglement entropies of fermionic systems, *Phys. Rev. A* **72** (2005) 022302, https://doi.org/10.1103/PhysRevA.72.022302
13. A. Grassi, A relationship between atomic correlation energy of neutral atoms and generalized entropy, *Int. J. Quantum Chem.* **111** (2011) 2390, https://doi.org/10.1002/qua.22541
14. L. Delle Site, On the scaling properties of the correlation term of the electron kinetic functional and its relation to the Shannon measure, *Europhys. Lett.* **88** (2009) 19901, https://doi.org/10.1209/0295-5075/88/19901
15. L. M. Ghiringhelli, L. Delle Site, R. A. Mosna and I. P. Hamilton, Information-theoretic approach to kinetic-energy functionals: the nearly uniform electron gas, *J. Math. Chem.* **48** (2010) 78, https://doi.org/10.1007/s10910-010-9690-6
16. N. Flores-Gallegos, Informational energy as a measure of electron correlation, *Chem. Phys. Lett.* **666** (2016) 62, https://doi.org/10.1016/j.cplett.2016.10.075
17. M. A. Nielsen and I. L. Chuang, Quantum Computation and Quantum Information *(Cambridge University Press, 2010)*,https://doi.org/10.1017/CBO9780511976667.
18. D. S. Naik, C. G. Peterson, A. G. White, A. J. Berglund and P. G. Kwiat, Entangled State Quantum Cryptography: Eavesdropping on the Ekert Protocol, *Phys. Rev. Lett.* **84** (2000) 4733, https://doi.org/10.1103/PhysRevLett.84.4733
19. M.-J. Zhao, S.-M. Fei, and X. Li-Jost, Complete entanglement witness for quantum teleportation, *Phys. Rev. A* **85** (2012) 054301, https://doi.org/10.1103/PhysRevA.85.054301
20. M. G. A. Paris, Quantum Estimation for Quantum Technology, *Int. J. Quantum Chem.* **07** (2009) 125, https://doi.org/10.1142/S0219749909004839
21. C. E. Shannon, A mathematical theory of communication, *Bell Sys. Tech. J.* **27** (1948) 379, https://doi.org/10.1002/j.1538-7305.1948.tb01338.x
22. R. González-Férez and J. S. Dehesa, Characterization of atomic avoided crossings by means of Fisher's information, *Eur. Phys. J. D* **32** (2005) 39, https://doi.org/10.1140/epjd/e2004-00182-3
23. A. Rényi, On Measures of Entropy and Information, *Berkeley Symposium on Mathematical Statistics and Probability* **4.1** (1961) 547 https://projecteuclid.org/ebook/Download?urlid=bsmsp/1200512181&isFullBook=false
24. C. Tsallis, Possible generalization of Boltzmann-Gibbs statistics, *J. Stat. Phys.* **52** (1988) 479,https://doi.org/10.1007/BF01016429
25. C. R. O. Onicescu, Possible generalization of Boltzmann-Gibbs statistics, *Hebd. Seances Acad. Sci. A* **263** (1966) 841, https://doi.org/10.1007/BF01016429
26. F. J. A. van Ruitenbeek, J. Goseling, H. W. Bakker, and A. A. K. Hein, Shannon Entropy as an Indicator for Sorting Processes in Hydrothermal Systems, *Entropy* **22** (2020) 656, https://doi.org/10.3390/e22060656
27. K.-W. Park, J. Kim, and S. Moon, Shannon Entropy as an Indicator of the Spatial Resolutions of the Morphologies of the Mode Patterns in an Optical Resonator, *Curr. Opt. Photon.* **5** (2021) 16 https://opg.optica.org/copp/abstract.cfm?URI=copp-5-1-16
28. S. Saha and J. Jose, Shannon entropy as an indicator of correlation and relativistic effects in confined atoms, *Phys. Rev. A* **102** (2020) 052824, https://doi.org/10.1103/PhysRevA.102.052824
29. R. González-Férez and J. S. Dehesa, Shannon Entropy as an Indicator of Atomic Avoided Crossings in Strong Parallel Magnetic and Electric Fields, *Phys. Rev. Lett.* **91** (2003) 113001, https://doi.org/10.1103/PhysRevLett.91.113001
30. Y. L. He, Y. Chen, J. N. Han, Z. B. Zhu, G. X. Xiang, H. D. Liu, B. H. Ma, and D. C. He, Shannon entropy as an indicator of atomic avoided crossings for Rydberg potassium atoms interacting with a static electric field, *Eur. Phys. J. D.* **69** (2015) 283, https://doi.org/10.1140/epjd/e2015-60397-7
31. C. Barrales-Martínez, R. Durán, and J. Caballero, Shannon entropy variation as a global indicator of electron density contraction at interatomic regions in chemical reactions, *J. Mol. Model.* **30** (2024) 371, https://doi.org/10.1007/s00894-024-06171-0
32. P. M. Cincotta *et al*., The Shannon entropy: An efficient indicator of dynamical stability, *Phys. D: Nonlinear Phenomena* **417** (2021) 132816, https://doi.org/10.1016/j.physd.2020.132816
33. H. W. Wijesekera and T. M. Dillon, Shannon entropy as an indicator of age for turbulent overturns in the oceanic thermocline, *J. Geophys. Res. Oceans* **102** (1997) 3279, https://doi.org/10.1029/96JC03605
34. J. P. Connerade, V. K. Dolmatov, and P. A. Lakshmi, The filling of shells in compressed atoms, *J. Phys. B: At., Mol. Opt. Phys.* **33** (2000) 251, https://dx.doi.org/10.1088/0953-4075/33/2/310

35. J. -P. Connerade, Confining and compressing the atom, *Eur. Phys. J. D* **74** (2020) 1, https://doi.org/10.1140/epjd/e2020-10414-y

36. D. Baye, Lagrange-mesh method for quantum-mechanical problems, *Phys. Stat. Sol. (b)* **243** (2006) 1095, https://doi.org/10.1002/pssb.200541305

37. P. Descouvemont, C. Daniel, and D. Baye, Three-body systems with Lagrange-mesh techniques in hyperspherical coordinates, *Phys. Rev. C* **67** (2003) 044309, https://doi.org/10.1103/PhysRevC.67.044309

38. M. Vincke, L. Malegat, and D. Baye, Regularization of singularities in Lagrange-mesh calculations, *J. Phys. B: At., Mol. Opt. Phys.* **26** (1993) 811, https://dx.doi.org/10.1088/0953-4075/26/5/006

39. L. G. Jiao, L. R. Zan, Y. Z. Zhang and Y. K. Ho, Benchmark values of Shannon entropy for spherically confined hydrogen atom, *Int. J. Quan. Chem.* **117** (2017) e25375, https://doi.org/10.1002/qua.25375

40. S. Mondal, A. Sadhukhan, K. Sen, and J. K. Saha, Structural properties and quantum information measures of H, Li and Na atoms endohedrally captured in C_{36} and C_{60} cages, *Eur Phys J. P.* **138** (2023) 576, https://doi.org/10.1140/epjp/s13360-023-04188-7